

Highlights

Reducing RES Droughts through the integration of wind and PV

Boris Morin, Aina Maimó Far, Damian Flynn, Conor Sweeney

- RES droughts are analysed using 45 years of hourly wind and PV generation data
- RES droughts from C3S-Energy and ERA5-Atlite datasets are compared
- Adding PV to a wind-dominated system reduces RES drought frequency and duration
- Validated RES datasets are crucial to accurately identify RES drought extremes

Reducing RES Droughts through the integration of wind and PV

Boris Morin^{a,*}, Aina Maimó Far^a, Damian Flynn^b, Conor Sweeney^a

^aSchool of Mathematics and Statistics, University College Dublin, Belfield, Dublin 4, Dublin, D04 V1W8, Ireland

^bSchool of Electrical and Electronic Engineering, University College Dublin, Belfield, Dublin 4, Dublin, D04 V1W8, Ireland

Abstract

The dependence of renewable energy sources (RES) such as wind and photovoltaic (PV) systems on the weather poses a critical challenge for energy systems. This study investigates the impact of targeting a balanced distribution of wind and PV capacity on reducing periods of low renewable generation, known as RES droughts. Three different RES models are used to estimate the capacity factors for different installed capacities of wind and PV energy. The skill of the RES models is quantified by comparing capacity factor time series to observed data. Their skill at representing RES droughts is also quantified. The RES models are used to generate a 45-year hourly time series of RES generation, enabling analysis of the frequency, duration and return periods of RES droughts at a climatological scale. Results show the importance of using an accurate, validated RES model for RES drought risk assessment. The addition of PV capacity to a wind-dominated system results in a large reduction in the frequency and duration of RES droughts, as well as reducing seasonal drought patterns. These findings underscore the importance of diversification in RES capacity to enhance energy security and resilience.

Keywords: RES Drought, Wind Power, Solar PV Power, Renewable Energy Sources, Return Periods

*Corresponding author

Email addresses: `boris.morin@ucdconnect.ie` (Boris Morin),
`aina.maimofar@ucd.ie` (Aina Maimó Far), `damian.flynn@ucd.ie` (Damian Flynn),
`conor.sweeney@ucd.ie` (Conor Sweeney)

1. Introduction

The EU aims to generate at least 69% of its electricity from renewable energy sources (RES) by 2030, up from 41% in 2022 (EuroStat, 2023). While this transition is essential for reducing greenhouse gas emissions, it also highlights the challenge of managing the variability of weather-dependent energy sources such as wind and photovoltaic (PV) power. This challenge is compounded by the increasing electrification of energy sectors, which places greater demand on the power system and makes it more sensitive to meteorological conditions (Bloomfield et al., 2016, 2021; van der Wiel et al., 2019). Periods of low renewable generation, known as *Dunkelflaute* or RES droughts, pose significant risks to system adequacy and energy security, emphasizing the need for a resilient energy system to meet both growing electricity demand and decarbonization targets.

This study focuses on Ireland, a region with a strong reliance on wind power, which has ambitious targets for PV power expansion. This case study provides valuable insights into the potential benefits of diversifying the renewable energy mix on RES droughts. The performance of different RES models are compared, and a 45-year time series of RES generation is produced. The results highlight the role of increased PV capacity in reducing RES drought risks, offering insights for policymakers and energy planners.

For this study, a RES drought event is defined as occurring when the average capacity factor (CF) remains below a fixed threshold for a given duration, following the methodology used in other research (Kaspar et al., 2019; Ohba et al., 2022; Mockert et al., 2023; Mayer et al., 2023). Alternative methods exist for defining RES droughts. One approach uses relative CF thresholds that change over the year to account for seasonal variations in renewable energy generation (Raynaud et al., 2018; Rinaldi et al., 2021; Gangopadhyay et al., 2022; Allen and Otero, 2023; Kapica et al., 2024). Another common method relies on percentile-based thresholds, where drought events are defined by identifying periods of unusually low generation relative to historical production levels, typically based on the lowest production percentiles (Bracken et al., 2024; Allen and Otero, 2023). Additionally, some studies combine these definitions with metrics that incorporate the demand side of energy consumption, analysing the balance between supply and demand during drought periods (Raynaud et al., 2018; Rinaldi et al., 2021;

36 Allen and Otero, 2023; Bracken et al., 2024). In this paper, the focus is
37 exclusively on energy generation, and a fixed threshold approach to define
38 RES droughts is used, which facilitates consistent inter-comparison between
39 scenarios with different installed wind and PV capacities.

40 RES droughts are identified using onshore wind and PV CF time series. In
41 this study, three different datasets are used, all of which are driven by ERA5
42 data (Hersbach et al., 2020). Two of the datasets are part of C3S Energy
43 (C3S-E) (, C3S), an energy-based operational dataset produced by the EU
44 Copernicus Climate Change Service (Dubus et al., 2023). One of the C3S-E
45 datasets provides CF time series aggregated at the national scale, while the
46 other provides the CF time series at each grid point, at the ERA5 resolution
47 of 0.25° . The third dataset was generated using the Atlite model (Hofmann
48 et al., 2021), which converts the ERA5 atmospheric data to a generation
49 time series using specified wind turbine and PV panel models. Atlite is an
50 open-source tool developed by PyPSA (Hofmann et al., 2021) and is widely
51 used for estimating wind and PV generation (Mockert et al., 2023; Li et al.,
52 2023; Parzen et al., 2023; Ali Khan Niazi and Victoria, 2023).

53 The datasets used in this study are detailed in section 2, which describes
54 their characteristics and relevance for evaluating RES droughts. Section 3
55 outlines the RES models used to simulate wind and PV generation and pro-
56 vides the methodology for defining and identifying RES drought events, in-
57 cluding the thresholds and metrics applied. In section 4, the models are first
58 verified against observed energy data to assess their accuracy, followed by an
59 analysis of RES drought occurrences for two scenarios with different ratios
60 of installed wind to PV capacities. Finally, section 5 offers a discussion of
61 the results in the context of energy reliability and future planning, followed
62 by the main conclusions and recommendations for further research.

63 2. Data

64 This study uses publicly available datasets to construct and validate the
65 models for estimating the CF of wind and PV energy. The primary data
66 sources include: EirGrid and SONI, the transmission system operators (TSO)
67 for the Republic of Ireland and Northern Ireland, respectively; the ERA5
68 reanalysis dataset; and the C3S-E datasets.

69 2.1. Wind and PV Capacity Factor

70 EirGrid, the TSO for the Republic of Ireland, and SONI, the Northern
71 Ireland TSO, provide detailed datasets on all wind and PV farms across the
72 island of Ireland (Republic of Ireland and Northern Ireland) from 1990 to
73 the present (SONI). These datasets include information such as each farm’s
74 installed capacity, name, and connection date. To enhance the accuracy of
75 this data, the longitude and latitude for each farm were manually determined
76 through online searches. For simplicity, this data will be referred to as orig-
77 inating from EirGrid, as all-island data was directly obtained from EirGrid,
78 and the combined regions of the Republic of Ireland and Northern Ireland
79 will be referred to as Ireland throughout the remainder of this document.

80 The spreadsheet available from the EirGrid website contains two key vari-
81 ables: generation and availability. Generation is the energy that a RES farm
82 actually contributed to the grid, which may include limitations introduced
83 by the TSO to maintain grid stability, such as constraints and curtailment.
84 Availability represents the energy that would have been generated from a
85 RES farm if no grid constraints had been applied, making it representative
86 of the weather-related response. Generation and availability values are avail-
87 able from 2014 onward for wind power and from 2018 onward for PV power,
88 although PV availability data only became present in the Republic of Ireland
89 in 2023. This study focuses on availability for all analyses.

90 2.2. Atmospheric Variables

91 Atlite and C3S-E datasets are driven by the ERA5 reanalysis (Hers-
92 bach et al., 2020), produced by the European Centre for Medium-Range
93 Weather Forecasts (ECMWF). This global gridded dataset provides hourly
94 atmospheric variables from 1940 to the present at a horizontal resolution of
95 0.25° . It is widely used for estimating PV and wind energy (Mockert et al.,
96 2023; Dubus et al., 2023; Brown et al., 2021; Otero et al., 2022). Table 1 lists
97 the ERA5 variables used by Atlite and C3S-Energy.

98 2.3. C3S Energy

99 The EU Copernicus Climate Change Service developed the C3S-E renew-
100 able energy dataset for Europe (Dubus et al., 2023), using ERA5 atmospheric
101 variables and weather-to-energy models. This dataset provides hourly CF for
102 wind and PV energy from 1979 to the present. The data are available on the
103 same grid as the ERA5 data, which has a horizontal resolution of 0.25° . The

Table 1: ERA5 variables used to calculate wind and PV generation

ERA5 name	variable
100 metre zonal and meridional wind speed	u_{100}, v_{100}
2 metre temperature	$t2m$
Surface net solar radiation	ssr
Surface solar radiation downwards	$ssrd$
Top of atmosphere incident radiation	$tisr$
Total sky direct solar radiation at surface	$fdir$

time series are also available for download at two aggregated scales: regional (NUTS 2) and national.

The C3S-E dataset estimates wind energy using wind speeds at 100 metres (u_{100}, v_{100}) and a standard turbine model, the Vestas V136/3450, with a fixed hub height of 100 meters. This choice is based on expert advice and the trend in wind turbine installation. The PV generation model used by C3S-E uses two ERA5 variables: surface solar radiation downwards ($ssrd$) and air temperature ($t2m$). PV generation is calculated multiple times, using the same model with different azimuth and tilt angles. The results are aggregated based on a statistical distribution of the module angles based on the geographical location (Saint-Drenan et al., 2018).

3. Methods

This study uses three datasets to analyse RES droughts across the island of Ireland. Data downloaded from C3S-E were used to obtain two datasets: one based on national-level data (C3S-E N), and another on grid-level data (C3S-E G). The third dataset was computed using the Atlite model (Atlite).

3.1. C3S-Energy National

For national-level analyses, the aggregated CF time series provided by C3S-E were used at two levels: Republic of Ireland (NUTS0: IE) and Northern Ireland (NUTS2: UKN0). These are based on the assumption by C3S-E that RES generation occurs at every ERA5 grid point in Ireland. We computed a weighted average of these, based on the installed capacity of each one, to represent the total CF for Ireland.

127 3.2. C3S-E Gridded

128 The gridded dataset from C3S-E was used to create CF datasets which
129 account for the location of RES farms in Ireland. A list of the RES farms in
130 Ireland was compiled, including each farm’s latitude, longitude and installed
131 capacity. Using these coordinates, the nearest grid point on the C3S-E grid
132 was identified for each farm. The CF values from the C3S-E dataset corre-
133 sponding to these grid points were retrieved. A weighted average of the CF
134 values was calculated, with the installed capacity of each farm serving as the
135 weight, to construct the CF time series for Ireland. This process resulted in
136 a time series of RES generation for each energy source (wind and PV) for
137 Ireland, which takes the location of the RES farms into account.

138 3.3. Atlite

139 Atlite transforms weather data into energy data using the gridded ERA5
140 data and the locations of existing RES farms, as described in C3S-E G.
141 ERA5 data for wind speed at 100 metres (u_{100} , v_{100}) are used to calculate
142 wind generation, while the ERA5 radiation variables (ssr , $ssrd$, $tisr$, and
143 $fdir$) and air temperature ($t2m$) are used to calculate PV generation. A
144 key distinction between C3S-E and Atlite lies in their representation of wind
145 turbines and PV panels. This study identifies the most appropriate wind
146 turbine power curve to use from the 121 power curves made available by
147 Renewables.ninja (Staffell and Pfenninger, 2016). The selection of a specific
148 wind turbine and PV panel characteristics is further discussed and explained
149 in section 4.1.

150 3.4. Energy Scenarios

151 In addition to analysing wind and PV generation separately, a combined
152 CF was computed for each model by averaging wind and PV generation,
153 weighted by their installed capacities at the end of 2023 (5.9 GW for wind
154 power and 0.6 GW for PV power). This configuration is referred to as the
155 91W-9PV scenario, reflecting the distribution of 91% wind and 9% PV ca-
156 pacity. Given that PV capacity in Ireland is low in 2023, and to explore how
157 a more balanced distribution of wind and PV capacities might impact RES
158 droughts, this study also considered a second scenario, referred to as 57W-
159 43PV, where the installed PV capacity is assumed to increase to 8.6 GW,
160 while wind capacity rises to 11.45 GW. These values are based on targets out-
161 lined in the roadmap published by the 2024 Climate Action Plan (of Ireland,
162 2023). This study does not include offshore wind in the analysis. Recent

163 reports suggest that even by 2030, Ireland is unlikely to have any significant
164 new offshore wind farms, with projected offshore capacity expected to remain
165 near zero using realistic scenarios (Ireland, 2024).

166 New time series were generated for both the Atlite and C3S-E G PV mod-
167 els, incorporating a revised distribution of installed capacity across Ireland
168 as specified in the roadmap. For wind power, the CF time series remains un-
169 changed, as significant shifts in the location of wind farms are not expected.
170 In total, twelve CF time series were analysed in this study, six for individual
171 wind and PV CF (three models for each source) in the 91W-9PV scenario,
172 and an additional six time series that include the combined CF for 91W-9PV
173 and 57W-43PV scenarios across the different models.

174 It is important to note that the specific capacity values used in this study
175 are illustrative and are not intended to reflect precise future realities. Instead,
176 they serve to explore the impact of transitioning from a wind-dominated sys-
177 tem (91W-9PV) to a more evenly distributed system (57W-43PV). This ap-
178 proach allows for a comparative analysis between the two scenarios, assessing
179 how the balance of RES capacity affects the occurrence of RES droughts.

180 3.5. *RES Drought Definition*

181 In this study, a RES drought event was defined as occurring when the 24-
182 hour moving average of CF remains below a fixed threshold of 0.1 for a period
183 of longer than 24 hours. The choice of this threshold is somewhat arbitrary,
184 but aligns with similar studies on low renewable energy production (Kaspar
185 et al., 2019; Ohba et al., 2022; Mayer et al., 2023). By using a 24-hour moving
186 average, fewer but longer-lasting events were captured compared to using the
187 raw CF time series, which can be more sensitive to short-term fluctuations.
188 A fixed threshold approach was chosen in this study to enable consistent
189 inter-comparison between datasets.

190 The moving average approach smooths out short-term fluctuations, so
191 that brief periods above the threshold do not interrupt an otherwise con-
192 tinuous low-CF period (Fig. 1). This means that a single hour above the
193 threshold does not "break" a drought event if it is surrounded by prolonged
194 low-generation hours. As a result, fewer but longer-lasting drought events
195 are identified, which may better reflect real-world conditions where energy
196 supply constraints persist over extended periods.

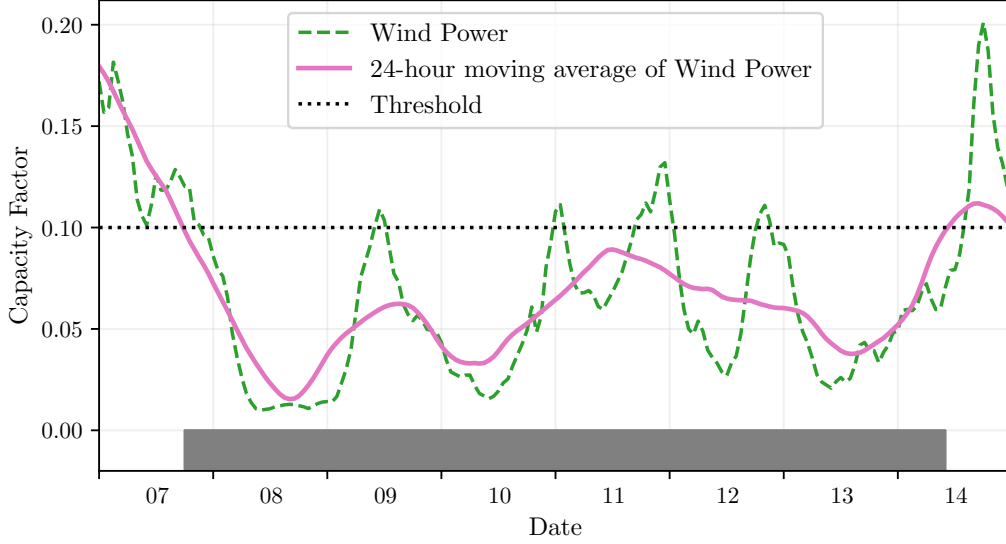


Figure 1: Wind time series of CF (green) and its 24-hour moving average (pink) from the 7th to the 15th of July 2021. The black dashed line indicates the CF threshold. The grey bar shows the period identified as a wind drought under our definition

197 4. Results

198 4.1. Verification

199 The accuracy of the datasets used in this study was verified, before con-
 200 tinuing to the analysis of RES droughts. For the verification process, time-
 201 varying values of installed capacity were used to account for changes in RES
 202 development over the verification period. This step allowed us to assess how
 203 well the datasets represent the production of renewable energy by comparing
 204 them against observed data.

205 4.1.1. Wind Energy

206 The C3S-E datasets use the Vestas V136/3450 wind turbine power curve,
 207 (Fig. 2a). The Atlite model allows the user to specify the power curve.
 208 We considered the 121 power curves available for download from Renew-
 209 ables.ninja (Staffell and Pfenninger, 2016). For each power curve, Renew-
 210 ables.ninja also provides four associated smoothed power curves. The smooth-
 211 ing is done using a Gaussian filter with different standard deviations that
 212 depend on the wind speed. A separate wind CF time series for Ireland was
 213 generated for each of the wind turbine power curves and smoothing levels.

214 The performance of each CF time series was then assessed based on four
 215 skill scores: correlation coefficient (CC), root mean square error (RMSE),
 216 mean bias error (MBE), and area under the curve. The area under the curve
 217 was calculated from histograms of the hourly CF values for the most recent
 218 decade, 2014-2023. Based on these metrics, the most representative power
 219 curve for Ireland was the Enercon E112.4500 power curve with the $0.3w$
 220 smoothing filter.

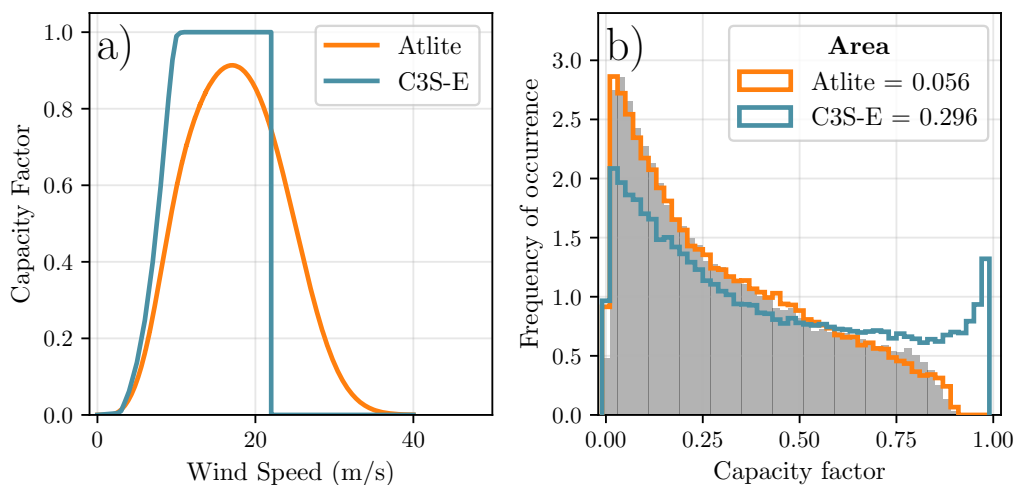


Figure 2: a) Power curves of the Enercon E112.4500 with a 0.3 smoothing filter used by Atlite (orange) and the Vestas V136/3450 used by C3S-E (teal) b) Histograms of wind CF for Ireland from Atlite (orange), C3S-E (teal) and Observed (shaded)

221 The smoothing of the wind turbine power curve represents losses associ-
 222 ated with each turbine, as well as losses such as wake effects between turbines,
 223 which are important when modelling wind energy on larger spatial scales.
 224 The histogram in Fig. 2b shows that the C3S-E power curve tends to under-
 225 estimate low CF values and overestimate higher ones, whereas the smoothed
 226 Atlite power curve more closely follows the recorded wind availability data
 227 from EirGrid.

228 The effect of the difference between the power curves is also visible in
 229 Fig. 3, which shows a density plot of wind CF values. The two C3S-E datasets
 230 are shown to overestimate the observed CF, whereas the Atlite model is in
 231 good agreement with the observed data. The skill scores presented in Table 2
 232 show that Atlite performs better than the C3S-E datasets for all of the skill
 233 scores.

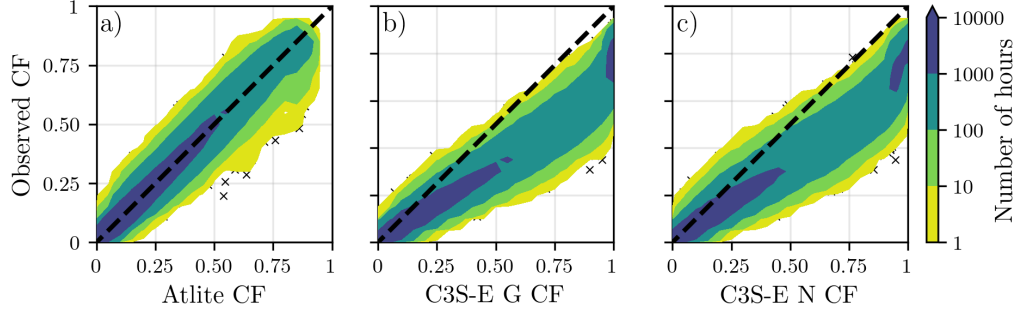


Figure 3: Wind CF density plot of the observed CF (vertical axes) and modelled (horizontal axes) CF data for the a) Atlite, b) C3S-E G and c) C3S-E N models

	Atlite	C3S-E G	C3S-E N
CC	0.981	0.972	0.970
RMSE	0.045	0.177	0.162
MBE	-0.003	0.137	0.121

Table 2: Skill scores for wind power for the three datasets compared to observed data

234 Fig. 4 presents the average annual number of wind drought events during
235 the 2014 to 2023 validation period. The figure presents that Atlite shows
236 the best agreement overall with the observed frequency and duration of wind
237 drought events. This pattern is particularly evident for shorter-duration
238 events, which are the most frequent.

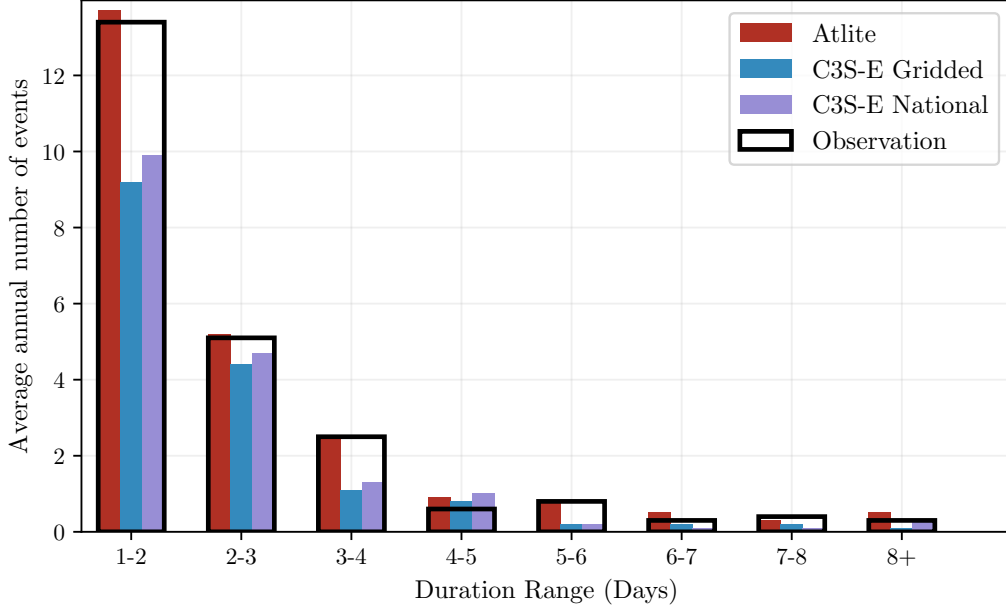


Figure 4: Average annual number of wind drought events for Atlite (red), C3S-E G (blue), C3S-E N (purple), and the observed data (black outline). The wind droughts are identified from 2014 to 2023

239 4.1.2. PV Energy

240 The Atlite model allows the user to select certain PV panel characteristics.
 241 In this study, the three PV panel types available in the Atlite model were
 242 considered (CSi, CdTe, Kaneka). Following the same methodology as in the
 243 previous section, the three available models were compared using four skill
 244 scores (CC, RMSE, MB, and area under the curve). Based on the best-
 245 performing metrics, the Breyer PV panel model was selected (Beyer et al.,
 246 2004), using the Kaneka Hybrid panel option. For all PV farm locations, the
 247 azimuth angle is fixed at 180°(due south), and the optimal tilt angle option
 248 is applied.

249 The PV installed capacity available on the spreadsheets from EirGrid
 250 represents the Maximum Export Capacity (MEC) and does not accurately
 251 reflect the installed PV capacity. To enable actual PV generation potential
 252 to be modelled correctly, installed capacities were set at 1.4 times the MEC
 253 values. This scaling factor was estimated by analysing proprietary data from
 254 individual PV farms provided by EirGrid, which showed that the installed

capacities of many farms exceed their MEC values by approximately 40%.

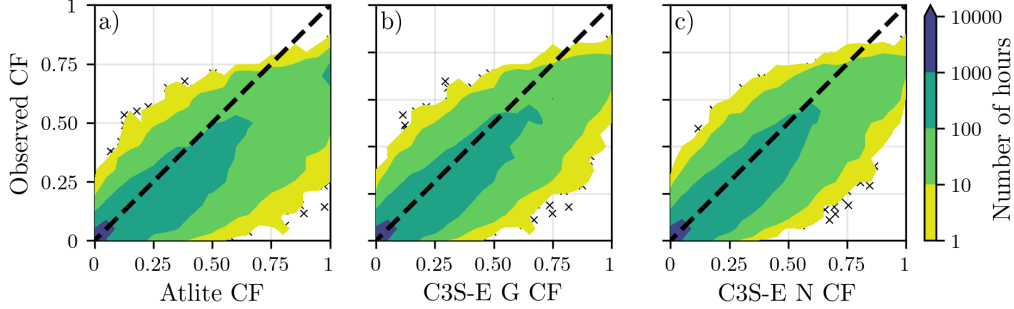


Figure 5: PV CF density plot of the observed (vertical axes) and modelled (horizontal axes) CF series for the a) Atlite, b) C3S-E G and c) C3S-E N models

Figure 5 shows that the three datasets have a similar tendency to overestimate the CF compared to the observed values, especially for high CF values. The skill scores presented in Table 3 indicate that C3S-E G performs best overall, with the lowest RMSE and a high correlation coefficient, suggesting a closer match to observed data. All models show a slight positive bias, with Atlite exhibiting a slightly lower correlation and higher RMSE.

	Atlite	C3S-E G	C3S-E N
CC	0.921	0.931	0.931
RMSE	0.119	0.090	0.113
MBE	0.046	0.027	0.021

Table 3: Skill scores for PV CF for the three datasets compared to observed data

Fig. 6 shows the number of PV drought events during the 2023 validation period across different duration ranges. The figure reveals partial agreement between the three datasets and the observed data, with consistent results noticed for duration ranges of 1-2, 3-4, 7-8, and 8+ days. However, discrepancies appear in the other ranges, where the models diverge from the observed data. The main challenge in validating PV data stems from the recent installation of a large share of Ireland's PV capacity, leading to uncertainties in PV generation data and the actual generating capacity in the first few months after each farm is connected. With over 65% of the total PV capacity installed in 2023, these data uncertainties significantly impact the ability to perform rigorous validation for PV drought events.

273 Nevertheless, the goal of this analysis is to assess the combination of wind
 274 and PV generation, where the complementary nature of these energy sources
 275 mitigates the limitations seen in PV-only results.

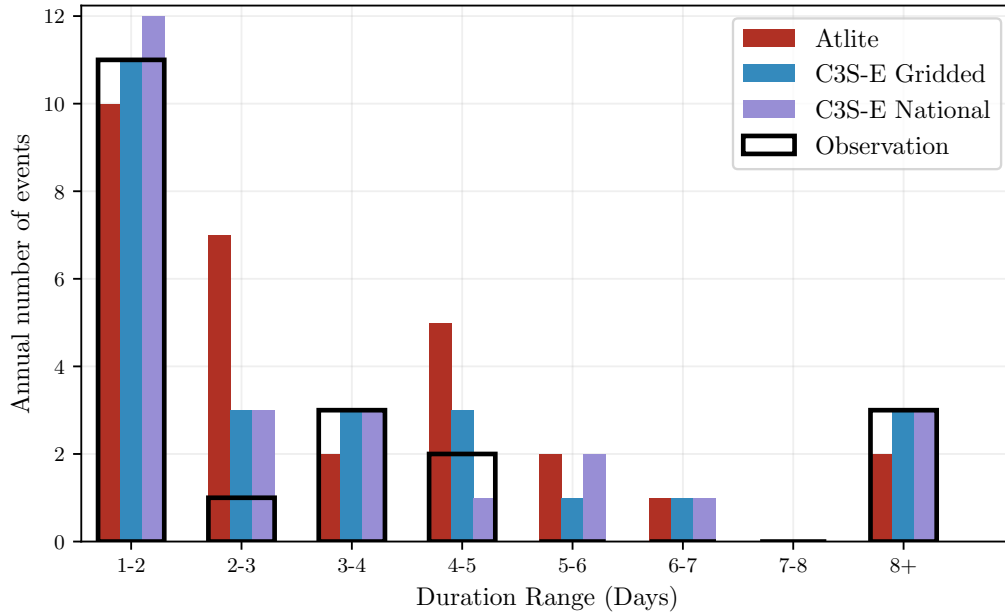


Figure 6: Number of PV drought events for Atlite (red), C3S-E G (blue), and C3S-E N (purple) and the observed data (black outline). The PV droughts are identified for 2023, considering the actual capacity of the system at any given time

276 4.2. Analysis

277 In this section, RES drought events are evaluated under two different
278 scenarios with fixed installed capacities: the 91W-9PV scenario, with 5.9 GW
279 of wind capacity and 0.6 GW of PV capacity, and the 57W-43PV scenario,
280 where wind capacity comprises 11.45 GW and PV capacity increases to 8.6
281 GW. Both scenarios were driven by 45 years of ERA5 data. Using the RES
282 drought identification process described in Section 3.5, wind and PV droughts
283 are first analysed separately before presenting the results for combined (wind
284 + PV) RES droughts under both scenarios.

285 4.2.1. Annual Number of RES Droughts

286 The first part of the analysis examines the annual number of RES drought
287 events across the three datasets. For Fig. 7a, the number of events decreases
288 as the duration range increases, with very few events lasting more than seven
289 days. For Fig. 7b, the number of events also declines as the duration range
290 extends from one to eight days, followed by a slight increase for longer dura-
291 tions. This increase is due to extended low-generation periods occurring from
292 November to March, depending on the dataset. When comparing wind and
293 PV results (Fig. 7a & b), the median, first, and third quartiles for PV are
294 consistently higher than or equal to those for wind, across all duration ranges
295 and datasets. This is due to the typically lower CF of PV power compared
296 to wind power, especially in a region such as Ireland where solar potential
297 is limited. PV generation is also zero at night and constrained by the daily
298 solar cycle, leading to a naturally higher frequency of RES droughts in PV
299 compared to wind.

300 Fig. 7a & b show the combination of wind and PV under the two capacity
301 scenarios. In the 91W-9PV scenario (Fig. 7c), the identified RES droughts
302 closely match those for wind alone, which is expected due to the dominance
303 of installed wind capacity. In contrast, the 57W-43PV scenario (Fig. 7d)
304 shows a clear reduction in the number of drought events across all datasets
305 and durations, with a decrease of the total number of events of 56% for Atlite,
306 52% for C3S-E G, and 50% for C3S-E N. This reduction is attributed to the
307 anti-correlation between wind and PV generation.

308 The median, first, and third quartiles for the Atlite dataset are consis-
309 tently greater than or equal to those of the other two datasets, regardless of
310 the duration range or type of renewable energy considered. This difference
311 arises from the wind turbine power curve model used in the C3S-E datasets,
312 which tends to overestimate the wind CF (Fig. 3). As a result, the overall

313 number of RES droughts is underestimated in the C3S-E datasets compared
 314 to Atlite.

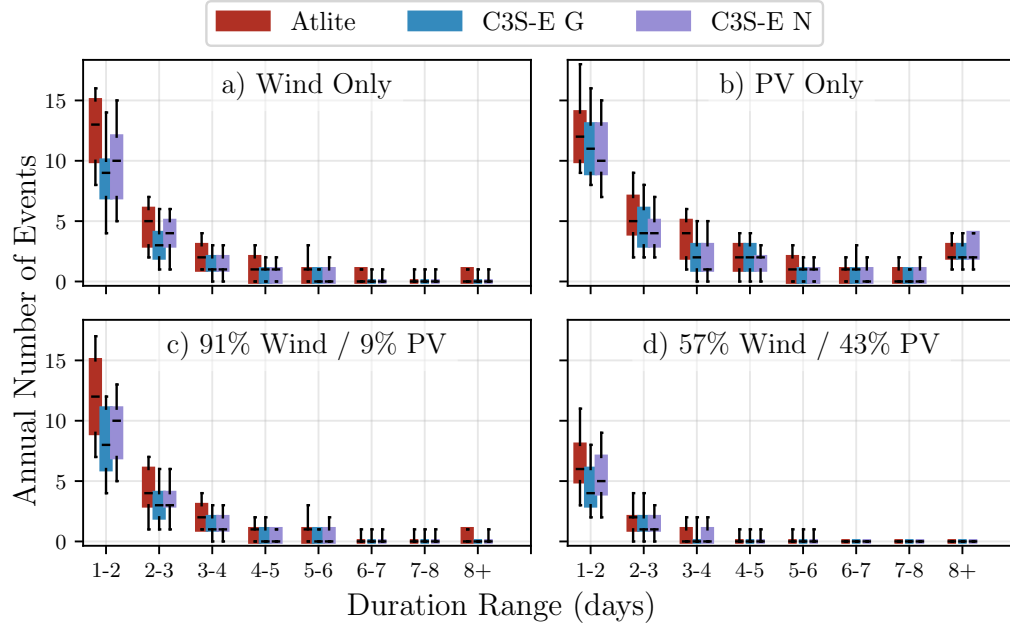


Figure 7: Annual number of RES droughts (from 1979 to 2023) for a) Wind, b) PV, and the combination for the c) 91W-9PV and d) 57W-43PV scenario for Atlite (red), C3S-E G (blue), and C3S-E N (purple). The x-axis represents duration ranges in days (lower bound included), while the y-axis indicates the annual number of events. The boxes display the first and third quartiles and the median is marked by a black line. The whiskers indicate the 5th and 95th percentiles

315 4.2.2. Return Periods of RES Drought Duration

316 The RES drought events identified over the 45-year period were used to
317 calculate the return periods for different RES drought durations. A return
318 period refers to the estimated expected interval between occurrences of events
319 with a specified duration or intensity. Fig. 8 illustrates the return periods
320 for varying RES drought durations, highlighting how often different drought
321 lengths are likely to occur across the datasets. This analysis provides insight
322 into the frequency and likelihood of prolonged low-generation periods, which
323 is crucial for evaluating the potential impact of RES droughts on energy
324 reliability and security of supply.

325 For wind (Fig. 8a), the duration of RES droughts increases in a log-
326 linear fashion across the three datasets. The log-linear trend indicates a pre-
327 dictable relationship between drought duration and occurrence, with longer
328 RES droughts becoming exponentially less likely as duration increases.

329 For PV (Fig. 8b), Atlite behaves differently than the two C3S-E datasets.
330 The Atlite results show a log-linear increase but reach higher values in general
331 with the longest event lasting forty days. For C3S-E G and C3S-E N, the
332 duration of RES droughts increases in a log-linear pattern for events lasting
333 less than 16 days. Beyond this duration, there is a sharp rise in drought
334 duration for events up to a one-year return period. This sudden increase
335 reflects the impact of winter on PV generation in Ireland, as PV output often
336 remains below the CF threshold for extended periods during winter months.
337 The difference between Atlite and the C3S-E results arises from differences in
338 the datasets near the threshold of 0.1 CF. Atlite remains slightly above the
339 threshold more frequently during these conditions, leading to shorter, more
340 fragmented drought events. In contrast, C3S-E G and C3S-E N tend to
341 fall below the threshold in similar conditions, resulting in longer continuous
342 drought periods, especially during winter. This sensitivity to the threshold
343 highlights how slight model differences can have substantial effects on drought
344 duration estimates, particularly for PV in low-generation conditions.

345 For the 91W-9PV scenario (Fig. 8c), the return periods mirror those of
346 Fig. 8a, due to the low levels of installed PV capacity. In the 57W-43PV
347 scenario (Fig. 8d), the return periods for RES droughts increase across all
348 durations. For example, the return period for a five-day drought event, shown
349 by the vertical dashed lines in Fig. 8, extends from roughly six months for
350 the 91W-9PV scenario, to four years for the 57W-43PV scenario in the Atlite
351 dataset, and from about fifteen months to around five years in the two C3S-E

352 datasets.

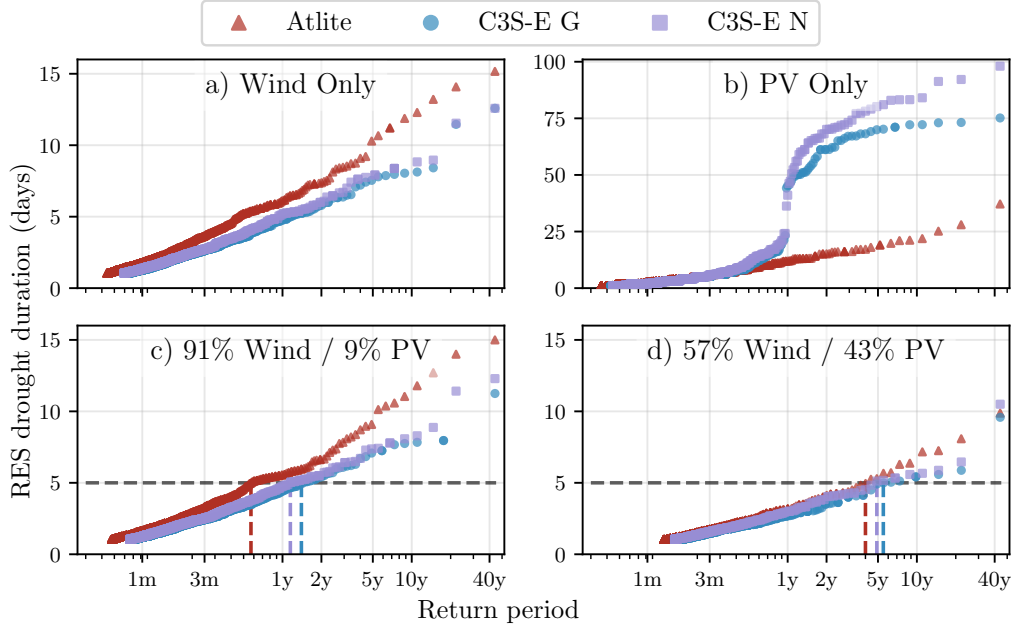


Figure 8: Return periods of the duration of RES droughts (from 1979 to 2023) for a) Wind, b) PV, and the combination for the c) 91W-9PV and d) 57W-43PV scenario, for Atlite (red triangle), C3S-E G (blue circle), and C3S-E N (purple square). The x-axis represents the return period time in a log-scale and the y-axis indicates the duration of RES drought associated with it. The horizontal dashed line marks the 5-day return period, with coloured vertical dashed marking its return period for each dataset

353 Across Fig. 8a, c, and, d, the return periods in the Atlite dataset are
 354 consistently higher than those in the two C3S-E datasets. For instance, in
 355 the 91W-9PV scenario (Fig. 8c), an event with a one-year return period
 356 lasts six days in the Atlite dataset, compared to only five days in the C3S-E
 357 datasets. This difference underscores the importance of model selection when
 358 quantifying RES droughts, as each model’s assumptions and parametrisations
 359 significantly influence drought duration estimates. Additionally, in all four
 360 graphs, the similarity between results from the two C3S-E datasets suggests
 361 that assumptions in the Atlite model—such as wind turbine power curve
 362 selection and PV panel specifications—have a greater impact on RES drought
 363 duration estimates than the precise geographic distribution of RES farms
 364 when studying the return periods of RES droughts.

4.2.3. Seasonal Distribution of RES Droughts

The seasonality of RES droughts was analysed by comparing the percentage of hours in each month classified as part of a RES drought.

For Fig. 9a, RES drought percentages are higher in summer than in winter. In the Atlite dataset, for instance, an average of 24% of hours in summer (June-July-August) are identified as RES droughts, compared to only 4% in winter (December-January-February). This seasonal variation is influenced by the wind power curve model used to estimate CF, where the shape of the curve in lower wind speed regions (3-10 m/s) leads to significant differences in CF under low wind conditions. In contrast, the results for Fig. 9b show a higher percentage in winter, with RES droughts occurring over 60% of the time regardless of the dataset. The Atlite results show a higher percentage of RES drought hours for wind, and a slightly lower percentage for PV, compared to the two C3S-E datasets.

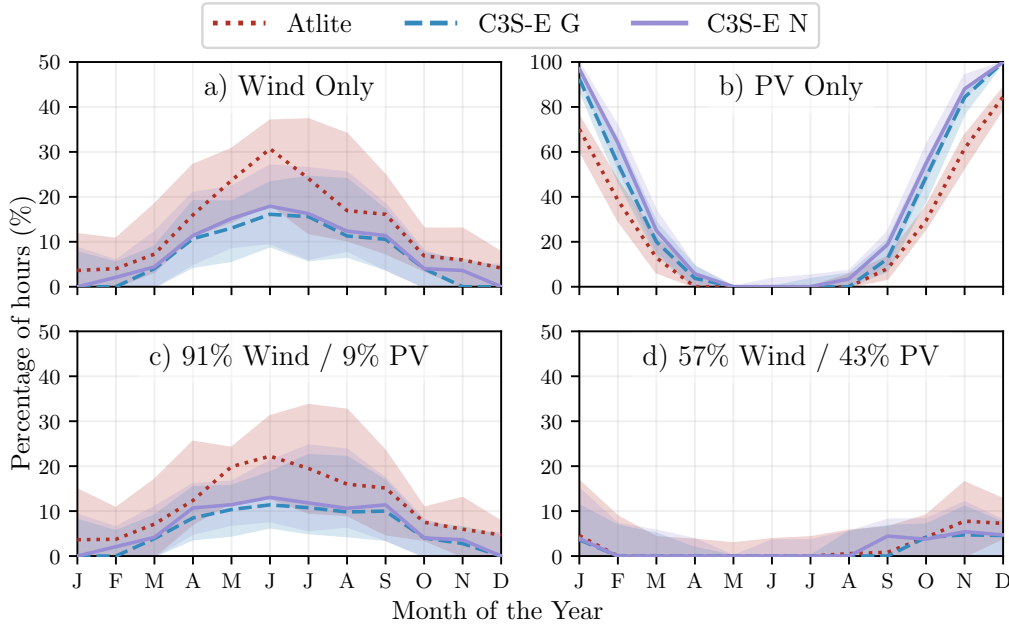


Figure 9: Percentage of hours in a month which are part of a RES drought (from 1979 to 2023) for a) Wind, b) PV, and the combination for the c) 91W-9PV and d) 57W-43PV scenario, for Atlite (red dotted), C3S-E G (blue dashed), and C3S-E N (purple solid). The x-axis represents the month of the year, and the y-axis indicates the percentage of hours. Lines correspond to the median values and the area between the first and third quartiles is shaded.

379 Similar to previous results, the 91W-9PV scenario (Fig. 9c) shows pat-
 380 terns comparable to 9a. However, in the 91W/9PV scenario, the number of
 381 hours classified as RES droughts in summer decreases slightly compared to
 382 the wind-only scenario. This reduction can be explained by the contribution
 383 of PV generation during the summer months in the 91W-9PV scenario, even
 384 though it constitutes only 11% of total capacity. Since the number of RES
 385 drought hours for PV in summer is near zero, this small contribution has a
 386 noticeable impact on reducing overall drought hours. In the 57W-43PV sce-
 387 nario (Fig. 9d), all three datasets show a reduction in monthly RES drought
 388 frequency. Annual reductions in median RES drought frequency are observed
 389 across the datasets, dropping from 14% to 5% for Atlite, from 8% to 3% for
 390 C3S-E G, and from 9% to 4% for C3S-E N. The balanced mix of wind and
 391 PV power in this scenario reduces the seasonal signal overall and significantly
 392 decreases the percentage of RES drought hours in the summer.

393 5. Discussion and Conclusions

394 This study has investigated the ability of three RES models to represent
395 RES droughts: Atlite, C3S-E G, and C3S-E N. One of the most evident dif-
396 ferences is how each dataset incorporates the specific locations of RES farms.
397 Both Atlite and C3S-E G consider the locations of wind and PV farms, which
398 should, in theory, provide a more accurate representation of RES generation.
399 While this approach slightly improves PV models, our analysis indicates that
400 for wind energy, the Atlite dataset performs better overall, especially in its
401 close alignment with observed data for wind generation estimates. This find-
402 ing suggests that, although the inclusion of RES farm locations is beneficial,
403 the accuracy of the RES model is more strongly influenced by underlying
404 model assumptions, such as selecting an appropriate wind power curve.

405 Atlite shows the best alignment with observed data for wind generation.
406 Differences between the models are smaller for PV, with C3S-G performing
407 marginally better than the other two. The results show that the two C3S-
408 E datasets (C3S-E G and C3S-E N) consistently yield similar outcomes,
409 indicating that their methodological differences have minimal impact. This
410 distinction was also evident in the analysis, where Atlite reported higher
411 return periods and a greater number of RES droughts, especially in scenarios
412 with a balanced share of RES. Again, the results from RES drought modelling
413 rely more on the precision of the wind power curve and PV panel models
414 than on the specific locations of RES farms. Atlite’s superior performance
415 highlights the importance of selecting validated models for assessing RES
416 drought risks. This careful model selection can better quantify risks, support
417 effective planning, and avoid the potential underestimation of capacity needs,
418 which is essential for ensuring energy security.

419 Looking at the 57W-43PV scenario, the analysis showed a significant im-
420 provement in the management of RES droughts due to the complementary
421 nature of wind and PV generation. Wind and PV together perform better
422 in terms of reducing drought frequency and duration than either would in-
423 dividually, largely because of the seasonal anti-correlation between the two
424 energy sources. This diversification reduces the seasonal impact on RES
425 droughts, as PV generation peaks in the summer and wind generation is
426 more consistent in winter. Ireland currently has a highly wind-dependent
427 energy system, but with ambitious targets for PV installations in the coming
428 years, the energy mix is expected to approach a balance between wind and
429 PV capacity. While this balanced approach offers a more stable and secure

energy supply by mitigating RES drought risks, it is important to note that having similar wind and PV capacities may not optimise other aspects, such as annual energy production or meeting nighttime loads. For policymakers, these findings underscore the importance of meeting these capacity targets to enhance energy security through diversification. Additionally, the choice of model for RES drought assessment becomes increasingly critical as more renewable capacity is integrated into the system.

Future work is planned to extend the current analysis. First, climate projection data will be integrated with different energy scenarios, incorporating the addition of offshore wind, to better understand how climate change might affect RES droughts. Second, expanding the geographic domain of the study to include the EU would provide a more comprehensive understanding of RES droughts in an interconnected energy grid. This would require extensive verification across all EU countries, making it a more complex but highly relevant challenge.

References

- Ali Khan Niazi, K., Victoria, M., 2023. Comparative analysis of photovoltaic configurations for agrivoltaic systems in europe. *Progress in Photovoltaics: Research and Applications* 31, 1101–1113.
- Allen, S., Otero, N., 2023. Standardised indices to monitor energy droughts. *Renewable Energy* 217, 119206. doi:10.1016/j.renene.2023.119206.
- Beyer, H.G., Heilscher, G., Bofinger, S., 2004. A robust model for the mpp performance of different types of pv-modules applied for the performance check of grid connected systems. *Eurosun* , 8.
- Bloomfield, H.C., Brayshaw, D.J., Shaffrey, L.C., Coker, P.J., Thornton, H.E., 2016. Quantifying the increasing sensitivity of power systems to climate variability. *Environmental Research Letters* 11, 124025.
- Bloomfield, H.C., Brayshaw, D.J., Troccoli, A., Goodess, C.M., De Felice, M., Dubus, L., Bett, P.E., Saint-Drenan, Y.M., 2021. Quantifying the sensitivity of european power systems to energy scenarios and climate change projections. *Renewable Energy* 164, 1062–1075. doi:10.1016/j.renene.2020.09.125.

462 Bracken, C., Voisin, N., Burleyson, C.D., Campbell, A.M., Hou, Z.J., Bro-
463 man, D., 2024. Standardized benchmark of historical compound wind and
464 solar energy droughts across the Continental United States. *Renewable*
465 *Energy* 220, 119550. doi:<https://doi.org/10.1016/j.renene.2023.119550>.

466 Brown, P.T., Farnham, D.J., Caldeira, K., 2021. Meteorology and cli-
467 matology of historical weekly wind and solar power resource droughts
468 over western North America in ERA5. *SN Applied Sciences* 3, 814.
469 doi:[10.1007/s42452-021-04794-z](https://doi.org/10.1007/s42452-021-04794-z).

470 (C3S), C.C.C.S., 2020. Climate and energy indicators for Europe from 1979
471 to present derived from reanalysis. doi:[10.24381/cds.4bd77450](https://doi.org/10.24381/cds.4bd77450). accessed
472 on 28-11-2024.

473 Dubus, L., Saint-Drenan, Y., Troccoli, A., De Felice, M., Moreau, Y., Ho-
474 Tran, L., Goodess, C., Amaro E Silva, R., Sanger, L., 2023. C3S Energy: A
475 climate service for the provision of power supply and demand indicators for
476 Europe based on the ERA5 reanalysis and ENTSO-E data. *Meteorological*
477 *Applications* 30, e2145. doi:[10.1002/met.2145](https://doi.org/10.1002/met.2145).

478 EuroStat, 2023. Renewable Energy Statistics.

479 Gangopadhyay, A., Seshadri, A.K., Sparks, N.J., Toumi, R., 2022. The
480 role of wind-solar hybrid plants in mitigating renewable energy-droughts.
481 *Renewable Energy* 194, 926–937. doi:[10.1016/j.renene.2022.05.122](https://doi.org/10.1016/j.renene.2022.05.122).

482 Hersbach, H., Bell, B., Berrisford, P., Hirahara, S., Horányi, A., Muñoz-
483 Sabater, J., Nicolas, J., Peubey, C., Radu, R., Schepers, D., et al., 2020.
484 The ERA5 global reanalysis. *Quarterly Journal of the Royal Meteorological*
485 *Society* 146, 1999–2049. doi:[10.1002/qj.3803](https://doi.org/10.1002/qj.3803).

486 Hofmann, F., Hampp, J., Neumann, F., Brown, T., Hörsch, J., 2021. Atlite:
487 a lightweight Python package for calculating renewable power potentials
488 and time series. *Journal of Open Source Software* 6, 3294.

489 of Ireland, G., 2023. Climate Action Plan 2024. 3.

490 Ireland, S.E.A., 2024. National Energy Projections 2024.

491 Kapica, J., Jurasz, J., Canales, F.A., Bloomfield, H., Guezgouz, M., De Fe-
492 lice, M., Kobus, Z., 2024. The potential impact of climate change on

493 european renewable energy droughts. *Renewable and Sustainable Energy*
494 *Reviews* 189, 114011. doi:10.1016/j.rser.2023.114011.

495 Kaspar, F., Borsche, M., Pfeifroth, U., Trentmann, J., Drücke, J., Becker,
496 P., 2019. A climatological assessment of balancing effects and shortfall
497 risks of photovoltaics and wind energy in germany and europe. *Advances*
498 *in Science and Research* 16, 119–128. doi:10.5194/asr-16-119-2019.

499 Li, J., Zhao, Z., Xu, D., Li, P., Liu, Y., Mahmud, M.A., Chen, D., 2023. The
500 potential assessment of pump hydro energy storage to reduce renewable
501 curtailment and co2 emissions in northwest china. *Renewable Energy* 212,
502 82–96.

503 Mayer, M.J., Biró, B., Szücs, B., Aszódi, A., 2023. Probabilis-
504 tic modeling of future electricity systems with high renewable energy
505 penetration using machine learning. *Applied Energy* 336, 120801.
506 doi:10.1016/j.apenergy.2023.120801.

507 Mockert, F., Grams, C.M., Brown, T., Neumann, F., 2023. Meteorological
508 conditions during periods of low wind speed and insolation in Germany:
509 The role of weather regimes. *Meteorological Applications* 30, e2141.

510 Ohba, M., Kanno, Y., Nohara, D., 2022. Climatology of dark doldrums
511 in japan. *Renewable and Sustainable Energy Reviews* 155, 111927.
512 doi:10.1016/j.rser.2021.111927.

513 Otero, N., Martius, O., Allen, S., Bloomfield, H., Schaeffli, B., 2022. Char-
514 acterizing renewable energy compound events across Europe using a lo-
515 gistic regression-based approach. *Meteorological Applications* 29, e2089.
516 doi:10.1002/met.2089. 13.

517 Parzen, M., Abdel-Khalek, H., Fedotova, E., Mahmood, M., Frysztacki,
518 M.M., Hampp, J., Franken, L., Schumm, L., Neumann, F., Poli, D., et al.,
519 2023. Pypsa-earth. a new global open energy system optimization model
520 demonstrated in africa. *Applied Energy* 341, 121096.

521 Raynaud, D., Hingray, B., François, B., Creutin, J., 2018. Energy droughts
522 from variable renewable energy sources in European climates. *Renewable*
523 *Energy* 125, 578–589. doi:https://doi.org/10.1016/j.renene.2018.02.130.

- 524 Rinaldi, K.Z., Dowling, J.A., Ruggles, T.H., Caldeira, K., Lewis, N.S.,
525 2021. Wind and Solar Resource Droughts in California Highlight the
526 Benefits of Long-Term Storage and Integration with the Western In-
527 terconnect. *Environmental Science and Technology* 55, 6214–6226.
528 doi:10.1021/acs.est.0c07848.
- 529 Saint-Drenan, Y.M., Wald, L., Ranchin, T., Dubus, L., Troccoli, A., 2018.
530 An approach for the estimation of the aggregated photovoltaic power gen-
531 erated in several European countries from meteorological data. *Advances*
532 *in Science and Research* 15, 51–62. doi:10.5194/asr-15-51-2018.
- 533 SONI, E., . System and Renewable Data Reports.
- 534 Staffell, I., Pfenninger, S., 2016. Using bias-corrected reanalysis to sim-
535 ulate current and future wind power output. *Energy* 114, 1224–1239.
536 doi:10.1016/j.energy.2016.08.068.
- 537 van der Wiel, K., Stoop, L.P., Van Zuijlen, B.R.H., Blackport, R., Van den
538 Broek, M.A., Selten, F.M., 2019. Meteorological conditions leading to
539 extreme low variable renewable energy production and extreme high en-
540 ergy shortfall. *Renewable and Sustainable Energy Reviews* 111, 261–275.
541 doi:10.1016/j.rser.2019.04.065.